



PerTPV – Perovskite thin film photovoltaics
Grant agreement 763977

D5.3

Tandem mini-module demonstrator (100 cm²) with 23% efficiency

WP5

Lead beneficiary: OXPV

Authors: CSEM, OXPV

Delivery date: 30 September 2021

Confidentiality level: Public



The PerTPV project has received funding from the European Union's Horizon 2020 research and innovation programme under grant agreement No 763977.

Revision History

| Author Name, Partner short name | Description | Date |
|--|--------------------|-------------|
| Adriana Paracchino, CSEM | Draft deliverable | 24/09/2021 |
| Matt Klug, OXPV | Revision 1 | 28/09/2021 |
| Adriana Paracchino, CSEM | Final version | 22/10/2021 |

Contents

| | |
|--|----------|
| REVISION HISTORY | 2 |
| CONTENTS..... | 2 |
| 1. OBJECTIVE | 3 |
| 2. INTRODUCTION..... | 3 |
| 3. TANDEM CELLS AND MINI-MODULES..... | 5 |
| 4. CONCLUSION | 8 |



1. Objective

The purpose of this deliverable is to demonstrate a large area tandem mini-module with a power conversion efficiency of 23%.

2. Introduction

Tandem mini-modules (MM) were made at CSEM in superstrate configuration using the stack reported in Figure 1.

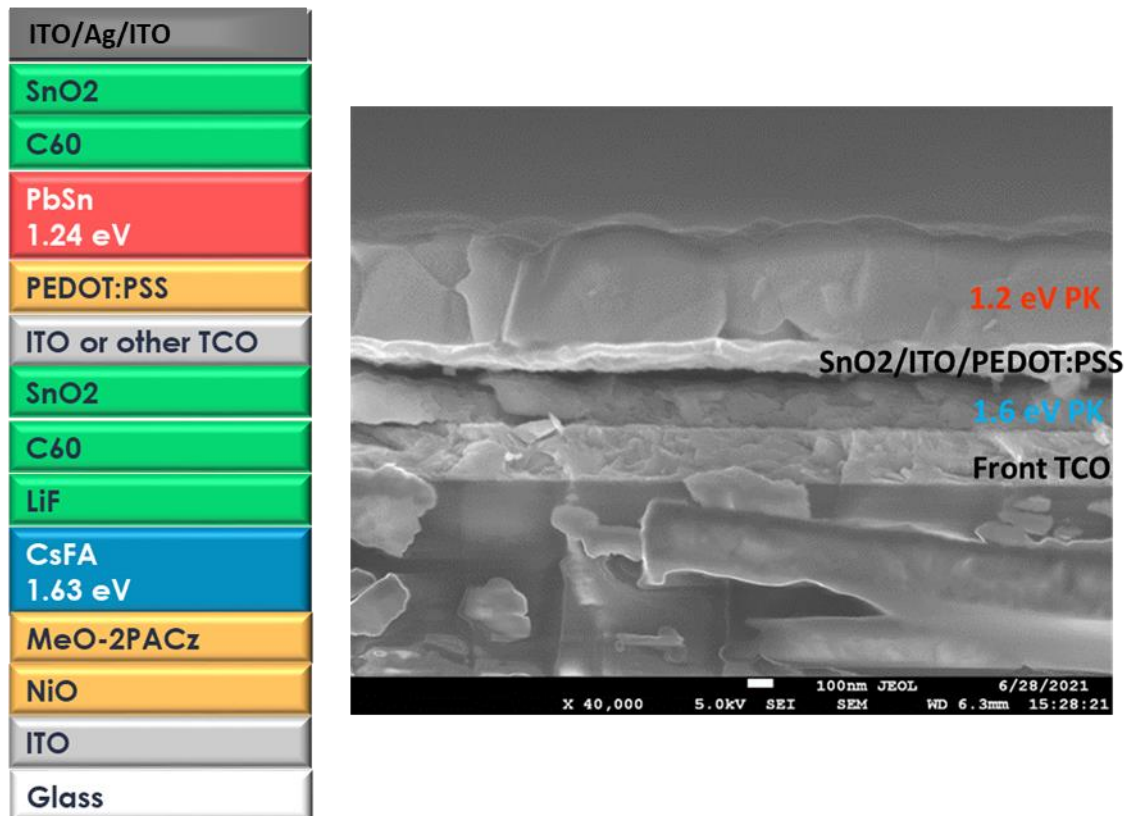
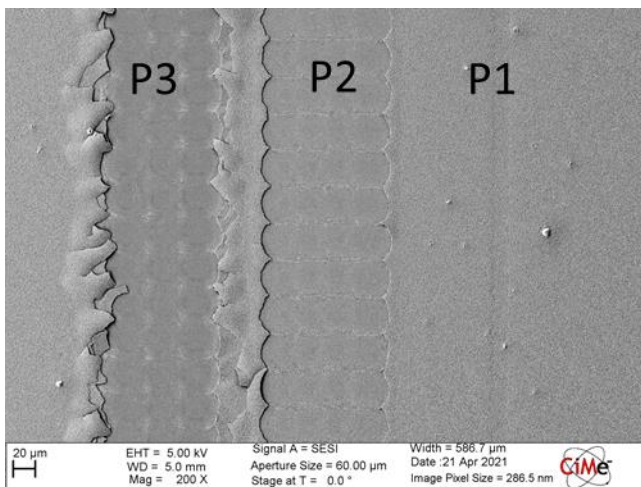
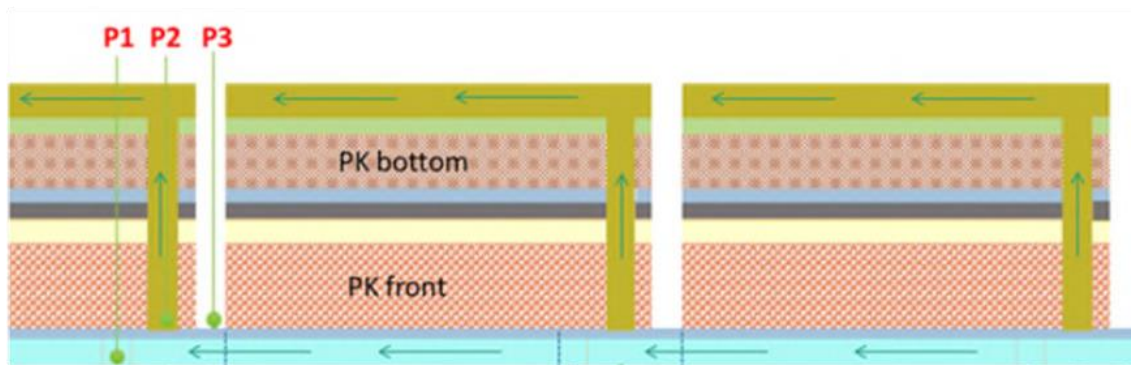


Figure 1. Stack of 2T tandems fabricated at CSEM and a cross-section SEM image

For the series interconnection of cells into mini-module CSEM employed the standard P1/P2/P3 laser scribing approach, which was already used in single-junction mini-module presented in D5.1. The interconnection design and a top view microscope image of the interconnection is shown in Figure 2.

Although the region between P1 and P3 is inactive and lowers the mini-module efficiency (expressed as aperture efficiency), we preferred to use large margins between the laser scribing lines in order to improve the number of functional modules. Moreover, taking into account the top electrode delamination around P3, the so-called “dead width” is about 300 μm .





P1~40 μm
 P2~130 μm
 P3~100 μm

Figure 2. Schematics of P1/P2/P3 series interconnection and SEM top view of the laser scribing lines. The area between P1 and P3 is inactive and does not contribute to the mini-module power.

A clear limitation of this interconnection design is the fact that the top electrode directly contacts the recombination layer TCO in the P2 line, thus potentially shunting the tandem. The presence of metal in P2, in direct contact with both perovskites, is also not desirable in terms of stability.

While more sophisticated interconnection approaches exist, for PerTPV we decided to use this approach, already available at CSEM, and tried to reduce the risk of shunting by increasing the sheet resistance of the recombination layer TCO.

As to the size of the mini-module, we preferred to use 5x5 cm² substrates rather than 10x10 cm² because they can still be processed by spin-coating, giving a direct comparison to the tandem 1 cm² cells. As a matter of fact, larger substrate sizes require either blade coating or slot-die coating, for which we observe somewhat lower performance yet, and also a stronger dependency of coating properties on the HTM used. Moreover, dynamic spin-coating of both HTM and low bandgap perovskite, in combination with a thick ALD SnO₂ layer below the recombination junction TCO, proved to be essential to avoid solvent damage on the wide bandgap perovskite. This may not be the case for blade-coating or slot-die coating as the films may take longer to dry.



In the CSEM mini-module, 5 cells are connected in series and the aperture area is 13.6 cm². As reported in D5.1, we observe only a minimal FF loss compared to 1 cm² cells.

3. Tandem Cells and Mini-modules

The performance of tandem mini-modules is directly related to the performance of tandem cells. As described in D3.7, the higher efficiency achieved at CSEM for the PK-PK tandem cells is 17% (on 1 cm²). This is then our target efficiency for the tandem mini-module.

Figure 3 shows the distribution of cells and mini-module efficiency made in the same batch, while Figure 4 shows the IV characteristics for the best MM and best cell of the batch. The recombination junction is a 10 nm thick ITO sputtered in presence of oxygen to achieve a sheet resistance of ~1000 ohm/sq.

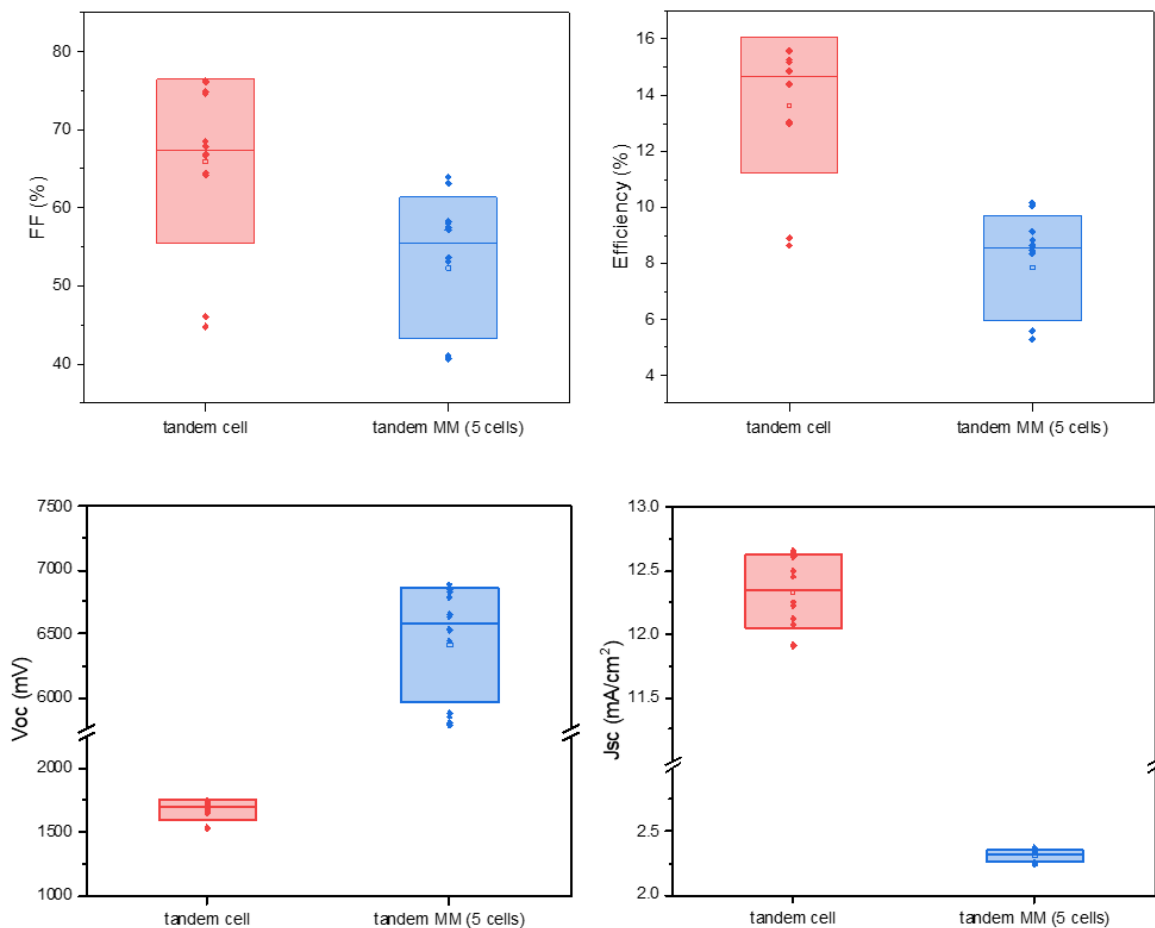


Figure 3. Statics of mini-module (MM) and cells fabricated in the same batch.

In this batch the best tandem cell reached only 15.6%. This was due to a thinner wide bandgap perovskite layer, which caused a current mismatch with the bottom cell (PbSn) of about 1 mA/cm². The control cells for the PbSn perovskite resulted in 11% average efficiency, which is quite a good value for CSEM.



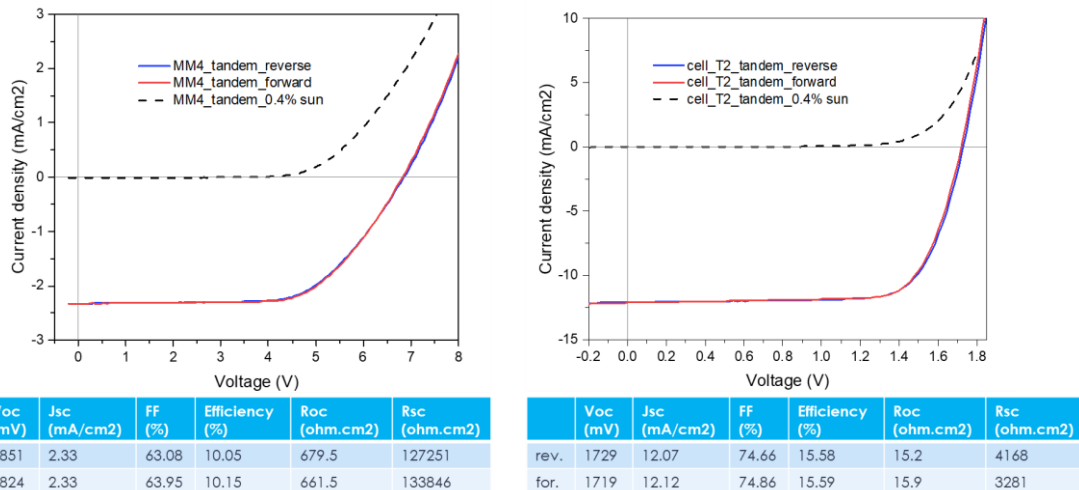


Figure 4. IV characteristics of the best 14 cm² tandem mini-module (left) and 1 cm² tandem cell (right) in the same batch.

In contrast to what we observe for single junction MM, a large FF drop occurs in tandem MM compared to tandem cells (from 75% to 64% for the best cell and MM, respectively). We can also see that the MM V_{oc} is not 5 times the V_{oc} of a single cell, as expected for series interconnection (6.8 V for the best MM, while 8.5 V was expected). We conclude then that there might be a shunting issue between the recombination junction ITO and the top electrode in the P2 line. Dark lock-in thermography (DLIT) is normally used to identify shunting paths in a cell, however it is less conclusive in the case of a MM as the current that is forced to flow through the narrow interconnection regions may induce confusion between series interconnection and shunts (Figure 5).

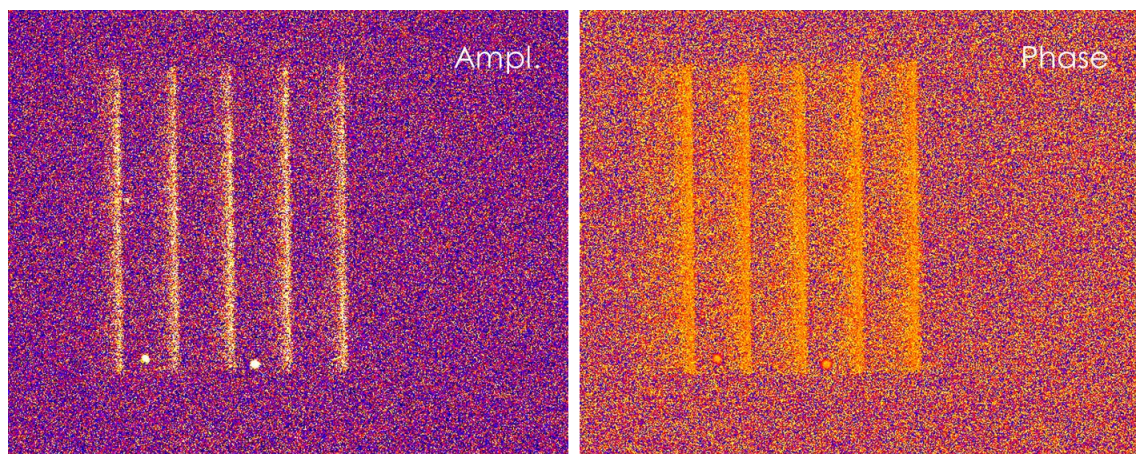


Figure 5. Amplitude and phase signal in dark lock-in thermography for one mini-module, showing the regions where the current flows as bright regions. While local shunts in the shape of dots are visible on the side of the MM, it is less clear whether shunts occur in the interconnections.

The resistive IV characteristics of the MM (Figure 4) may indicate the presence of some residues in the P2 scribing line or perhaps a discontinuous rear contact at the bottom of the P2 line. We checked these hypotheses by doing a cross-sectional FIB-SEM (Figure 6). Layer delamination is strongly reduced when preparing a cross section by FIB compared to mechanically cleaving a sample, however some delaminated regions are noticeable. In Figure 6 it looks like the rear electrode is quite thin and perhaps



discontinuous at the bottom of the P2 line but this could also be an artefact occurred during the cross-section preparation by FIB.

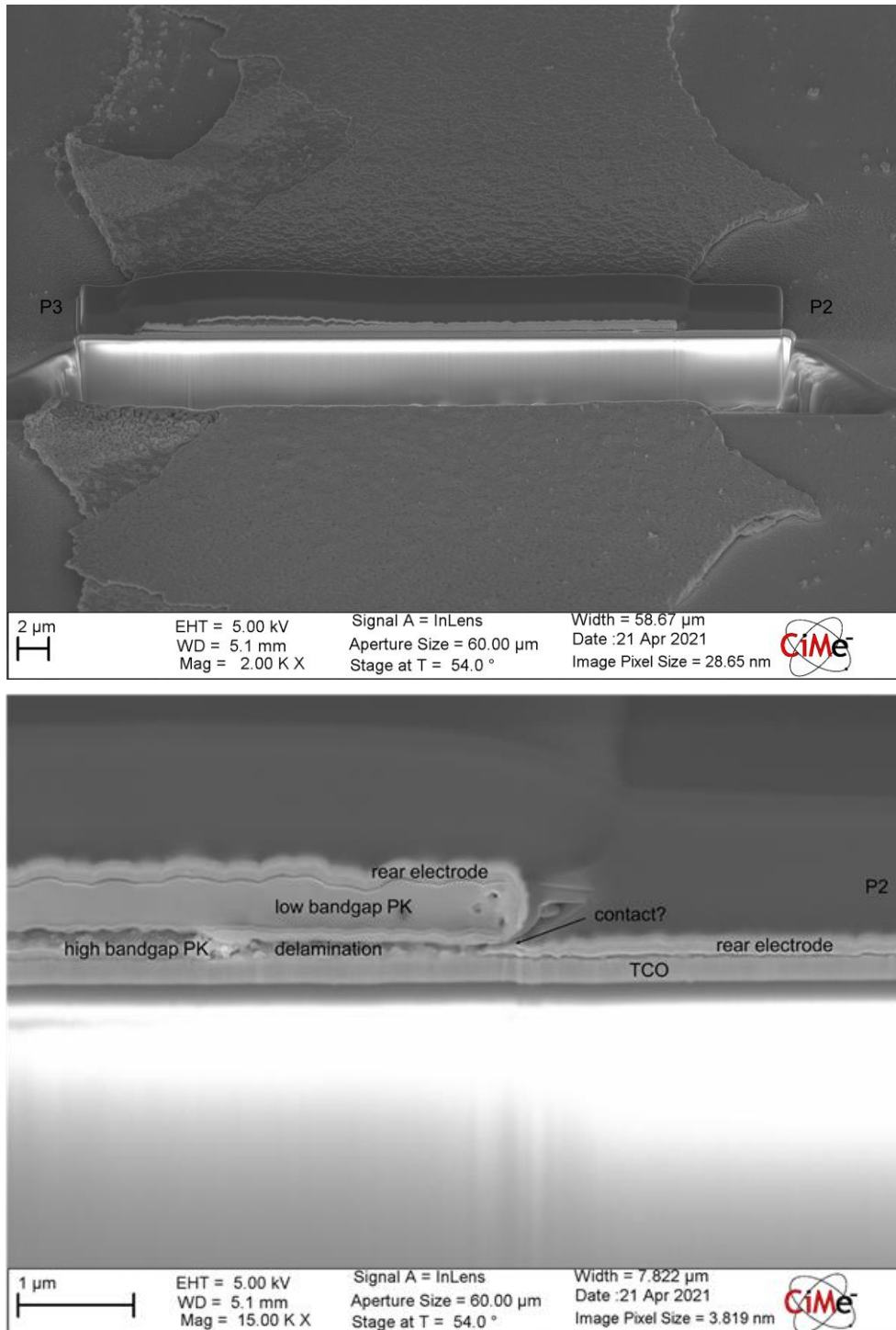


Figure 6. A FIB cross section in the region between P2 and P3 lines (top) and a zoom-in on the P2 line.



We have attempted to replace the ITO recombination junction by a more resistive AZO but we observed a strong S-shape in the IV characteristics of the tandem cells. Replacing the ITO with islands of silver (nominally, a layer of 1 nm thickness) strongly reduced both V_{oc} and J_{sc} . Therefore, we tried to increase the resistance of the ITO recombination layer by reducing the sputtering power and maximising the oxygen flow, which resulted in an increased sheet resistance of about 2 orders of magnitude. Surprisingly, while the tandem cell efficiency increased of $\sim 1.5\%$ absolute, the mini-module FF and V_{oc} did not show any improvement. Further batches of mini-module were particularly poor in terms of efficiency, mainly due to a suboptimal PbSn perovskite performance.

4. Conclusion

We have developed a superstrate-based two-terminal all-perovskite tandem device build and have successfully integrated it into a 14 cm^2 mini-module demonstrator (assembled on a $5 \times 5\text{ cm}^2$ substrate) through implementing a P1/P2/P3 interconnection approach. The champion mini-module achieved a power conversion efficiency of 10% and an additive open-circuit voltage of 6.8 V for 5 serially connected 2T tandem cells. This demonstrates the feasibility of modularising an all-perovskite multi-junction device through serial interconnection. We expect that overcoming the bottlenecks that limit the photovoltaic performance for the PbSn bottom sub-cell would yield immediate gains in future mini-modules built with this methodology. Further development of the interlayer or interconnection methodology is expected to mitigate sub-cell shunting and unlock the full additive voltage that should be achievable in future all-perovskite multi-junction mini-modules.

